Journal of Nano- and Electronic Physics
Vol. **15** No 2, 02018(4pp) (2023)

Журнал нано- та електронної фізики
Том **15** № 2, 02018(4cc) (2023)

Structural and Optical Properties of $Ba(Zr_{0.3}Ti_{0.7})O_3$ and $Ba(Zr_{0.5}Ti_{0.5})O_3$ Thin Films Prepared by Sol-Gel Method

Rahmi Dewi, T.S. Luqman, Krisman, A.S. Rini, H. Yanuar*

Department of Physics Universitas Riau, 28132 Pekanbaru, Indonesia

(Received 05 December 2022; revised manuscript received 23 April 2023; published online 27 April 2023)

$BaZr_xT_{1-x}O_3$ (BZT) thin film with $x = 0.30$ and 0.50 has been prepared with FTO glass substrate using a sol-gel method with an annealing temperature of 600 °C for one hour. BZT thin films are characterized using XRD and UV-vis to analyze their structural and optical properties. XRD spectra analysis of BZT thin films for the composition $x = 0.3$ and 0.5 crystal structure obtained is perovskite tetragonal. It has good crystals, while the diffraction angle 2θ would increase as the Zr content increase. The optical properties of BZT thin films were also analyzed, where the absorbance value increased with increasing Zr content at a wavelength of 300 – 375 nm. The band gap energy increases when composition (x) increases, and the highest band gap energy for composition $x = 0.5$ is about 3.54 eV.

Keywords: $BaZr_xT_{1-x}O_3$ thin film, Sol-gel method, Crystal structure, Energy gap

DOI: 10.21272/jnep.15(2).02018 PACS numbers: 77.55.f, 78.20.Ci

1. INTRODUCTION

Researchers mostly use lead-free materials in ferroelectric research on thin film technology, and the closest material is $BaTiO_3$ [1]. The Zr^{4+} doped with BT material can improve ferroelectric and piezoelectric properties [2]. Chemically, Zr^{4+} has a higher level of stability than Ti^{4+} because Zr^{4+} inhibits conduction by electrons moving between Ti^{4+} ions [3]. $BaTiO_3$ material can reduce the curie's temperature by doping the Zr^{4+}. The Tc reduction optimum value in $BaZr_xTi_{1-x}O_3$ material is at composition $x = 0.6$, as reported by Muhsen et al., in 2020 [4]. However, a large composition will cause a phase change from tetragonal to cubic. Therefore, it is necessary to vary the Zr composition in order to have a good level of tetragonality [5]. Many researchers have developed BZT ferroelectrics, one of which is the BZT capacitor in the form of a thin film. Because the thin film will form a very thin layer in micro size which is able to make the surface area larger, and the charge storage will be larger in quantity, which results in the larger capacitance value of the capacitor [6]. The increase in the capacitance value of the capacitor can also be increased by adding a dielectric material to the capacitor. The BZT is a ferroelectric dielectric material with spontaneous polarization in the absence of an external electric field [7].

In this study, the preparation of $BaZr_xT_{1-x}O_3$ thin films with $x = 0.30$, and 0.50 used the sol-gel method, and the samples were spin coated at a speed of 3600 rpm to obtain an optimum thinness level. As reported by Priya et al. (2020), a speed of 3600 rpm was able to make better and flatter thin film level [8]. Samples that have been spin-coated will head to the furnace stage with 600 °C annealing temperatures for 1 hour. Furthermore, it is known that the heating conditions using the furnace greatly affect the phase formation, crystal structure, and optical properties of these BZT thin film samples. The crystal size increases, and the particle morphology changes from spherical to cube with increased annealing temperature [9].

In this paper, we report the optical properties of $Ba(Zr_xTi_{1-x})O_3$ thin film, with $x = 0.30$ and 0.50 at FTO substrates with XRD and UV-vis spectroscopy in the wavelength range 300 – 800 nm.

2. EXPERIMENT

The BZT solution preparation using the sol-gel method can be carried out with the following chemical equation:

$$BaCO_3 + ZrCO_{2(x)} + Ti_{(1-x)}O_2 \rightarrow BaZr_{(x)}Ti_{(1-x)}O_3 + 2CO$$

Therefore, $BaZr_xTi_{1-x}O_3$ with with $x = 0.30$, 0.55, 0.60, and 0.50 in the form of a solution dripped on a glass substrate and then spin-coated at a speed of 3600 rpm for 30 seconds. Further, heated in an oven at 150 °C for 30 minutes and pre-annealed at 300 °C for 30 minutes. The following step was the annealing process. Samples were annealed with 600 °C temperature variations for 1 hour, and then, the samples were characterized using XRD and UV-vis Spectroscopy.

3. RESULTS AND DISCUSSIONS

XRD characterization is carried out to see the formation of the BZT crystalline phase or a new phase on the surface of the FTO substrate, as well as to determine the influence of variations in composition (x). The crystal plane indexing is based on the Crystallography Open Database (COD) database No. 96 – 210 – 7060 using match 3! software. Fig. 1 shows the BZT thin-film XRD spectrum for the $x = 0.3$ composition having a crystalline orientation plan (100), (110), (111), and (200) with a reflection angle of $2\theta = 22.78°$; 32,17°; 38.42° and 47.73° while for compositions $x = 0.5$ it also has a crystalline orientation plan (100), (110), (111) and (200) with slightly different diffraction angles of $2\theta = 22.58°$; 31,98°; 38.22°

* yanuar.hamzah@lecturer.unri.ac.id

and 47.53°. Our study showed that the XRD peaks of thin film BZT were similar as reported by the literature [10]. The increase in Zr percentage content results in the angle of 2θ shifting on the same plane. The shift in reflection angle 2θ due to Zr will occupy Site-B in the ABO_3 perovskite structure so that site-B changes phase from cubic to tetragonal [10]. From empirical data, Zr atoms have atomic radii of 155 pm, while Ti has an atomic radius of 140 pm. The large Zr atomic radius of Ti increases site-B size in the perovskite structure, which results in the scattering of X-ray Diffraction undergoing a shift received by the detector in the XRD characterization process [11].

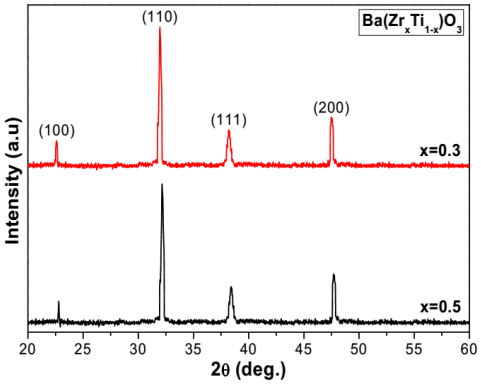

Fig. 1 – XRD spectra of BZT thin films with composition at $x = 0.3$ and 0.5

The BZT thin films for composition $x = 0.3$ and 0.5 crystal structure obtained is tetragonal as shown in Table 1, where lattice parameters $a = b$ is not equal to c. Increasing Zr content increases the d space, where the diffraction peak shifts towards the lower diffraction angle [12]. The lattice parameters and the volume of cell units increase with decreasing diffraction angles. Cubic phase and tetragonal angle diffraction are almost similar, the calculated lattice parameters and crystal size are listed in Table 1.

Table 1 – The $BaZr_xTi_{1-x}O_3$ crystal parameters and size with composition at $x = 0.3$ and 0.5 at the 600 °C annealing temperature

x	Lattice Parameters			Crystal Size (nm)
	a (Å)	c (Å)		a (Å)
$x = 0.30$	4.00	4.24	$x = 0.30$	4.00
$x = 0.50$	3.95	4.14	$x = 0.50$	3.95

A good degree of crystallinity is indicated by the large value of the crystal size in the BZT thin films has been reported by ref [13]. As shown in Table 1, the crystal size at the 600 °C annealing temperature with composition $x = 0.30$ and $x = 0.50$ has a crystal size decreases with the increased Zr. BZT crystal size can be calculated using Debye Scherrer equation; the full width half maximum (FWHM) value is taken from the highest diffraction peak in the crystal plane (110) with an FWHM value of 0.24 ($x = 0.3$) and 0.36 ($x = 0.5$). The crystal size of the BZT sample was 344.5 and 349.3 nm. Peak shift at a lower diffraction angle $2\theta = 0.2°$ indicates an increase in lattice parameters due to ionic radii Zr^{4+} ($r_{Zr^{4+}} = 0.86$ Å) > ionic radius Ti^{4+} ($r_{Ti^{4+}} = 0.74$ Å) and, therefore, replacement of Ti^{4+} with Zr^{4+} may increase BZT thin film lattice parameters [12], as seen in Fig. 2. From the width of the peak (110), which is more intense, a Gaussian fitting is used to determine the FWHM.

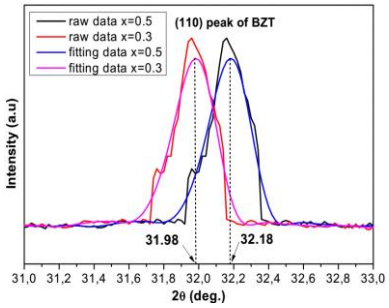

Fig. 2 – XRD spectra of BZT thin films peak shift (110) at a lower diffraction angle

UV-vis spectra of ZnO BZT thin films with composition at $x = 0.3$ and 0.5 at a wavelength of 300 – 800 nm. The absorbance spectrum is shown in Fig. 3. This BZT thin film has an absorbance value at 300 – 375 nm wavelength. The maximum absorbance value is at the smallest wavelength, having a minimum value at a wavelength of 400 – 800 nm.

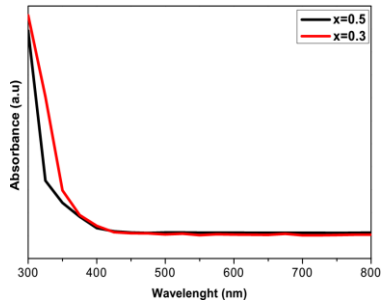

Fig. 3 – Absorban spectra of BZT thin films with composition at $x = 0.3$ and 0.5

The absorbance value increases with the increased Zr composition at a wavelength of 300 – 375 nm. Zr atom has a radius larger than the Ti atom and can absorb more light [14]. Therefore, a large composition has a large concentration, so the absorbance value also increases because the absorbance is directly proportional to the concentration of Zr.

The transmittance value in Fig. 3 is inversely proportional to the absorbance value. The maximum transmittance value is at a wavelength of 400 – 800 nm.

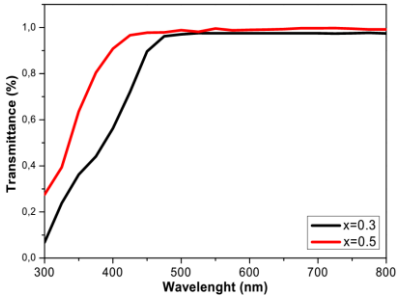

Fig. 4 – Transmittance spectra of BZT thin films with composition at $x = 0.3$ and 0.5

The transmittance value increases with the decreased Zr composition at a wavelength of 400 – 800 nm. The increased Zr composition causes more Zr atoms than Ti [15]. A large number of atoms makes it difficult for light to pass through because of the absorption of the amount of light, as described [16]. Therefore, the transmittance value increases with the decreased Zr composition. The relationship between transmittance and sample concentration is also inversely proportional, as explained in the "Lambert Beer" formula. Therefore, a large composition has a large concentration, so the transmittance value will decrease due to the amount of light absorption compared to the transmitted light [17].

Fig. 4 shows the band gap energy value obtained using the tauc plot method. The energy obtained is a graph between $(\alpha hv)^2$ versus (hv). The BZT energy band gap was 3.37 and 3.54 eV for $x = 0.3$ and $x = 0.5$ calculated using the Tauc plot, which results similar to the BZT energy gap band reported in the literature [18]. The small energy gap at the composition $x = 0.3$ is influenced by the grain size and crystal size of the BZT samples. The grand crystal size will indicate that the crystal structure is uniform. The density of the arranged atoms causes the conduction band to approach the valence band [17]. Therefore, the BZT energy band gap for the composition $x = 03$ is smaller than $x = 0.5$ at the 600 °C annealing temperature. This BZT thin film has an increasing optical band energy gap with an increase in Zr content from 3.37 to 3.54 eV. However, the BZT optical band gap obtained is more than the barium titanate ($BaTiO_3$) thin films by the CBD method, the optical band gap value is 3.31 eV [19]. As reported by ref [16] this smaller energy band gap explained that Zr doping into the BT structure causes stress relaxation of the lattice parameters so that the energy band gap becomes lower. It is also stated in reference [20] higher Zr dopant in the perovskite phase can cause defects such as oxygen vacancies.

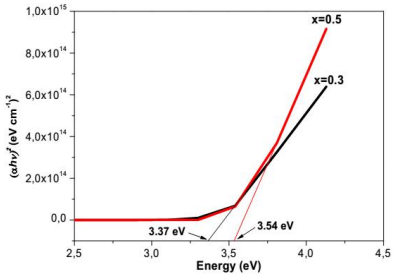

Fig. 5 – Tauc Plot of absorbance spectra of the BZT thin films with composition at $x = 0.3$ and 0.5

Table 2 shows the thickness, refractive index, and energy gap of the BZT thin films. The BZT thin at the composition $x = 0.3$ has a thickness larger than the composition $x = 0.5$. The Zr composition effect on the BZT thin film thickness is inconsistent. The thickness inconsistency may be due to the BZT liquid unevenly dripping on the glass substrate. One of the optical properties of thin films is the refractive index (n). Then for the calculation of the value of n, we use the following empirical formula by Herve and Vandamme [21].

Table 2 – The thickness, refractive index, and band gap energy of BZT thin films with composition at $x = 0.3$ and 0.5

x	Thickness (m)	Refractive index	E_g (eV)
0.30	3.37×10^{-7}	2.24	3.37
0.50	3.06×10^{-7}	2.41	3.54

The BZT thin film refractive index for $x = 0.3$ is 2.24 and $x = 0.5$ is 2.41, and the difference is not significant with the increase in Zr content. In this study, it was found that there is a difference in the refractive index between $BaZr_{0.3}Ti_{0.7}O_3$ and $BaZr_{0.5}Ti_{0.5}O_3$ films. The $BaZr_{0.3}Ti_{0.7}O_3$ film refractive index is smaller than the $BaZr_{0.5}Ti_{0.5}O_3$. Lie et al. [13], reported that the substitution of Zr in the $BaTiO_3$ structure would drive a decrease in the extinction coefficient of the thin film BZT, which corresponds to the chemical stability of Zr^{4+} ions. The $BaZr_{0.3}Ti_{0.7}O_3$ and $BaZr_{0.5}Ti_{0.5}O_3$ thin film refractive indices are about 2.24 and 2.41, while that value near the single crystal refractive index $BaTiO_3$ is about 2.3 [21].

4. CONCLUSSIONS

Current work is devoted to understanding the structural and optical properties of Ba $(Zr_xTi_{1-x})O_3$ (BZT) thin films with ($x = 0.30$ and $x = 0.5$) prepared with the sol-gel method. BZT perovskite phase has a relatively high structural stability level. Substitution using Zr^{4+} cation is possible. Furthermore, the lattice parameter $Ba(Zr_xTi_{1-x})O_3$ thin film, with $x = 0.30$ (4.24 Å) and $x = 0.50$ (4.14 Å) more significant than $BaTiO_3$ (~ 3.99 Å), prompted engineering to create this film thickness grown on FTO substrates. Finally, analysis of structural and optical properties BZT is a potential ferroelectric material for piezoelectric applications.

ACKNOWLEDGMENTS

This study was supported by Department of Physics, Faculty of Mathematics and Natural Sciences University of Riau, Indonesia.

REFERENCES

1. S. Sahoo, S. Hajra S, Manojit, M. De, R.N.P Choudhary, *Ceram. Int.* **44**, 4719 (2018).
2. J.P. Jwala, O. Subohi, M.M. Malik, *Mater. Res. Exp.* **6**, 096308 (2019).
3. A.E. Souza, G.S. Sasaki, S.A. Camacho, S.R. Teixeira, M.S. Li, E. Longo, *J. Lumin.* **17**, 132 (2016).
4. K.N.D.K. Muhsen, R.A.M. Osman, M.S. Idris, *J. Mater. Sci.: Mater. Electron.* **32**, 12771 (2021).
5. T. Badapanda, S. Sarangi, B. Behera, P.K. Sahoo, S. Anwar, T.P. Sinha, G.E. Luz, E. Longo, L.S. Cavalcante, *Curr. Appl. Phys.* **14** 708 (2014).
6. W. Huang, Y. Chen, X. Li, G. Wang, N. Liu, S. Li, M. Zhou, X. Dong, *Appl. Phys. Lett.* **113**, 203902 (2018).
7. Q. Wei, M. Zhu, L. Li, Z. Guo, M. Zheng, Y. Hou, *J. Alloy. Compd.* **731**, 631 (2018).
8. A. Sathiya Priya, D. Geetha, T. Ştefan, *Mater. Lett.* **281**, 128615 (2020).
9. J. Petzelt, D. Nuzhnyy, M. Savinov, V. Bovtun, M. Kempa,

T. Ostapchuk, J. Hlinka, G. Canu, V. Buscaglia, *Ferroelectrics* **469**, 14 (2014).
10. V.K. Veerapandiyan, M. Deluca, S.T. Misture, W.A. Schulze, S.M. Pilgrim, S.C. Tidrow, *J. Am. Ceram. Soc.* **103** 287 (2020).
11. S. Engelhardt, C. Molin, S. Gebhardt, S. Fähler, K. Nielsch, R. Hühne, *Energy Technol.* **6**, 1526 (2018)
12. A. Dixit, S.B. Majumder, A. Savvinov, R.S. Katiyar, R. Guo, A.S. Bhalla, *Mater. Lett.* **56**, 933 (2002).
13. L. Aiyun, X. Jianqiang, M. Xiangjian, S. Jinglan, H. Zhiming, C. Junhao, *Appl. Surf. Sci.* 254, 5660 (2008).
14. W. Cai, C. Fu, J. Gao, X. Deng, *J. Mater. Sci. Mater. Electr.* **21**, 796 (2010).
15. J. Shukla, S. Bisen, M. Khan, A. Mishra, *AIP Conf. Proc.* **2115**, 030194 (2019)
16. A. Kheyrdan, H. Abdizadeh, A. Shakeri, M.R. Golobostanfard, *J. Sol-Gel Sci. Technol.* **86**, 141 (2018).
17. V. Kavitha, P. Mahalingam, M. Jeyanthinath, N. Sethupathi, *Mater. Today: Proc.* **23**, 12 (2020).
18. L. Jin, J. Qiao, L. Wang, L. Hou, R. Jing, J. Pang, L. Zhang, X. Lu, X. Wei, G. Liu, Y. Yan, *J. Alloy. Compd.* **784**, 931 (2019).
19. K. Sidra, H. Nudrat, N. Saba, R. Saira, A. Shahid, N. Shahzad, *J. Mater. Res. Technol.* **9**, 11439 (2020).
20. M.K. Mahata, T. Mondai, C. Brüsewitz, K. Kumar, V.K. Rai, H. Hofsässa, U. Vettera. *Phys. Chem. Chem. Phys.* **17**, 20741 (2015).
21. P.J.L. Herve, L.K.J. Vandamme, *Infrared Phys. Technol.* **35**, 609 (1994).
22. E.D. Palik, *Handbook of Optical Constants of Solids A* (Academic, New York: 1991).

Структурні та оптичні властивості тонких плівок $Ba(Zr_{0.3}Ti_{0.7})O_3$ та $Ba(Zr_{0.5}Ti_{0.5})O_3$, отриманих золь-гель методом

Rahmi Dewi, T.S. Luqman, Krisman, A.S. Rini, H. Yanuar

Department of Physics Universitas Riau, 28132 Pekanbaru, Indonesia

Тонкі плівки $BaZr_xT_{1-x}O_3$ (BZT) з $x = 0.30$ і 0,50 були виготовлені на скляній підкладці FTO за допомогою золь-гель методу з температурою відпалу 600 °C протягом однієї години. Для аналізу структурних і оптичних властивостей тонких плівок BZT застосовували методи XRD та UV-vis. Отримана кристалічна структура перовскіту з тетрагональною решіткою. Він має хороші кристали, тоді як кут дифракції 2θ збільшиться зі збільшенням вмісту Zr. Також були проаналізовані оптичні властивості тонких плівок BZT, де значення поглинання зростало зі збільшенням концентрації Zr на довжині хвилі 300-375 нм. Енергія забороненої зони збільшується зі збільшенням концентрації x, і найбільша енергія забороненої зони для складу $x = 0.5$ становить близько 3,54 еВ.

Ключові слова: Тонкі плівки $BaZr_xT_{1-x}O_3$, Золь-гель метод, Кристалічна структура, Ширина забороненої зони.